www.czasopisma.pan.pl PAN POLSKA AKADEMIA NAUK www.journals.pan.pl

VERSITA

Arch. Min. Sci., Vol. 58 (2013), No 1, p. 269–282

Electronic version (in color) of this paper is available: http://mining.archives.pl

DOI 10.2478/amsc-2013-0019

MARIUSZ WADAS*

METHOD FOR DETERMINATION OF THE RANGE OF FAILURE ZONE AROUND MACROCRACKS SURFACE IN ROCK MEDIUM

METODA BADANIA ZASIĘGU STREFY ZNISZCZENIA WOKÓŁ POWIERZCHNI MAKROPĘKNIĘĆ W OŚRODKU SKALNYM

In this work a method, developed by the author, of microscopic investigations of deformation structures occurring in rock medium is presented. This method is based on adoption of multi-stage complex procedure encompassing numerous diverse examinations and measurements. As a result of following this method, information about geometrical features of microfractures and microfissures distribution (coordinates, length, occurrence frequency and directions of propagation) is obtained, which in turn allow to determine the range and intensity of destruction zones around macroscopic fissures in investigated samples. Testing was performed on selected three samples of the Tumlin Sandstone (three microscopic sections), representing the following states of stress-strain:

sample no. 1 (σ_3 = 200 MPa confining pressure and ε_1 = 5% longitudinal strain)
sample no. 2 (σ_3 = 300 MPa confining pressure and ε_1 = 10% longitudinal strain)
sample no. 3 (σ_3 = 300 MPa confining pressure and ε_1 = 15% longitudinal strain)

On the basis of conducted research it has been stated that increasing confining pressure $\sigma_3 = \sigma_2$ results in the increase of number and range of microfissures occurrence. At confining pressure $\sigma_3 = \sigma_2$ 200 MPa and longitudinal strain ε_1 = 5% a zone of intensive fracturing is noticeable, reaching about 6mm from the surface of macroscopic fracture. However, at higher confining pressure and higher longitudinal strains ($\sigma_3 = \sigma_2$ 300 MPa and ε_1 = 10% as well as $\sigma_3 = \sigma_2$ 300 MPa and ε_1 = 15%) microcracks and microfissures cover almost whole volume of the sample.

Keywords: confining pressure, rock mass, slip surface, microcracks, stress, strain

W artykule przedstawiono opracowaną przez autora metodę badań mikroskopowych struktur deformacji występujących w ośrodku skalnym. Metoda ta polega na zastosowaniu wieloetapowej złożonej procedury obejmującej wiele różnorodnych badań i pomiarów. W wyniku jej przeprowadzenia uzyskuje się informacje o geometrycznych cechach rozkładu mikrospękań i mikroszczelin (współrzędne, długość, częstość występowania i kierunki rozprzestrzenienia), które z kolei pozwalają na określenie zasięgu i intensywności strefy zniszczenia wokół pęknięć makroskopowych w badanych próbkach. Do badań zastosowano grubo ławicowy dolno triasowy piaskowiec pochodzący z północnej części obrzeżenia Gór

* CENTRAL MINING INSTITUTE, PLAC GWARKÓW 1, 40-166 KATOWICE, POLAND

Świętokrzyskich z okolic Tumlina. Piaskowiec charakteryzuje się zmienną barwą, od czerwono-brunatnej do jasnobrązowej, drobnym i średnim uziarnieniem oraz spoiwem krzemionkowo-żelazisto-ilastym. Głównym składnikiem skały są dobrze obtoczone miejscami ostrokrawędziste ziarna kwarcu o średnicy od 0,1 do 1,0 mm (średnio 0,5 mm).

Badania właściwości mechanicznych piaskowca tumlińskiego wykonano w Pracowni Odkształceń Skał Instytutu Mechaniki Górotworu PAN w Krakowie. Badania piaskowca przeprowadzono na próbkach cylindrycznych o średnicy 22,5 mm i dwukrotnie większej wysokości w trójosiowym stanie naprężeń, pod zmiennym ciśnieniem okólnym w zakresie od 0 do 400 MPa. Próbki piaskowca początkowo poddano działaniu wszechstronnego hydrostatycznego naprężenia $\sigma_1 = \sigma_2 = \sigma_3$, które odpowiadało zadanemu ciśnieniu okólnemu, a następnie przy stałej wartości tego ciśnienia, próbki obciążano siłą osiową do zadanej z góry wartości odkształcenia podłużnego. Badania wykonano w kilkunastu cyklach. Jeden cykl obejmował przeprowadzenie badań dla czterech próbek piaskowca pod stałym ciśnieniem okólnym i zadanym z góry zmiennym odkształceniem podłużnym dla każdej próbki innym wynoszącym 5%, 10%, 15% i 20%. Po uzyskaniu przez próbkę wymaganego odkształcenia podłużnego, odciążano ją do wartości zerowej naprężenia różnicowego następnie wyciągano ją z komory ciśnieniowej aparatu, szczegółowo oglądano i fotografowano. Z uzyskanych podczas badań przebiegu krzywych w układzie naprężenie różnicowe względem odkształcenia podłużnego i poprzecznego (rys. 2.) wynika, iż przy zwiększającym się ciśnieniu okólnym wzrasta wytrzymałość próbki oraz odpowiadające jej odkształcenia podłużne i poprzeczne. Poniżej wartości 200 MPa ciśnienia okólnego próbki pękały krucho, a pęknięcie poprzedzone było odkształceniami sprężystymi i niewielkimi odkształceniami trwałymi. Pęknięcie to było raptowne i towarzyszyły mu efekty akustyczne. Dla ciśnień okólnych – powyżej 200 MPa – próbki charakteryzowały się ciągliwym charakterem niszczenia, lecz zanim zaczęły pękać, osiągały znaczne odkształcenia.

Próbki piaskowca po wykonanych badaniach w trójosiowym stanie naprężeń spojono w żywicy epoksydowej w celu utrwalenia powstałych deformacji (pęknięć i szczelin). Żywica epoksydowa zabarwiona kolorem niebieskim, migrując przez strukturę próbek skalnych, wypełniła pustki – pory i szczeliny powstałe podczas badań trójosiowych. Spojony piaskowiec pocięto na fragmenty – plastry (grubości kilku milimetrów), równolegle do osi pionowej próbek z których przygotowano szlify mikroskopowe. Badania mikroskopowe szerokiej gamy szlifów, autor przeprowadził przy pomocy mikroskopu optycznego firmy „Olympus" zintegrowanym z cyfrowym aparatem fotograficznym. Dla charakterystycznych obszarów w obrębie szlifów mikroskopowych wykonano serie kolorowych zdjęć fotograficznych w 25 i 100 krotnym powiększeniu. Na podstawie przeprowadzonej analizy rozwoju mikroskopowych struktur deformacji w próbkach piaskowca wyróżniono dwa typy niszczenia materiału skalnego. W pierwszym typie zniszczenia, części materiału nie objęte pęknięciem są wolne od zniszczeń, jedynie w bezpośrednim sąsiedztwie strefy pęknięcia (powierzchni ścinania) występują mikropęknięcia i mikroszczeliny. Próbka jest ścinana skośnie do podstawy, a kąt nachylenia powierzchni pęknięcia względem podstawy próbki wykazuje tendencję malejącą ze wzrostem ciśnienia okólnego. W drugim typie zniszczenia, powstały intensywnie spękane strefy. Skupienia mikropęknięć i mikroszczelin wyraźnie rozprzestrzeniają się w znacznej objętości próbki. Różnica między dwoma typami zniszczenia uwidoczniła się także w liczebności i zasięgu mikropęknięć i mikroszczelin występujących w sąsiedztwie powierzchni pęknięć oraz intensywnie spękanych stref (pasm).

Do badań mikroskopowych struktur deformacji metodą komputerowej analizy obrazu fotograficznego, wytypowano trzy próbki piaskowca (trzy szlify mikroskopowe piaskowca) odpowiadające następującym stanom naprężeniowo-odkształceniowym:

próbka nr 1 (σ_3 = 200 MPa ciśnienia okólnego i ε_1 = 5% odkształcenia podłużnego)
próbka nr 2 (σ_3 = 300 MPa ciśnienia okólnego i ε_1 = 10% odkształcenia podłużnego)
próbka nr 3 (σ_3 = 300 MPa ciśnienia okólnego i ε_1 = 15% odkształcenia podłużnego)

Na podstawie przeprowadzonych obserwacji mikroskopowych wydzielono dla w/w szlifów obszary z charakterystycznymi strefami rozwoju spękań i wykonano dla nich serię kolorowych zdjęć fotograficznych, tworzących profile pomiarowe. W profilach pomiarowych zarejestrowano wszystkie mikroszczeliny. Zdjęcia wykonano w powiększeniu 100-krotnym, prostopadle do osi pionowej próbki, tak aby stykając się ze sobą obejmowały ciągłe przejście z obszarów pozbawionych pęknięć lub obszarów nieznacznie zniszczonych, w strefy ze spękaniami obejmującymi powierzchnie poślizgu. Profile pomiarowe obejmowały swym zasięgiem fragment powierzchni szlifu mikroskopowego o długości około 11 mm i wysokości 1,0 mm.

Przygotowanie danych wejściowych do analizy komputerowej wykonano w dwóch etapach.

W etapie pierwszym zeskanowano zdjęcia z profili pomiarowych, a następnie za pomocą programu Photo Shop wydzielono struktury deformacji.

W etapie drugim zastosowano program Scion Image, za pomocą którego dla ogółu wydzielonych mikroszczelin określono następujące parametry:

- numer porządkowy mikroszczeliny,
- współrzędne x, y środka mikroszczeliny,
- długość mikroszczeliny,
- wartość kąta zawartego pomiędzy kierunkiem rozprzestrzenienia się mikroszczeliny a powierzchnią poślizgu

W efekcie przetwarzania danych, program Scion Image nadaje każdej wydzielonej mikroszczelinie numer porządkowy. Program skanuje powierzchnie przetworzonego obrazu, następnie zlicza wydzielone mikroszczeliny przyporządkowując im kolejny numer. Program oblicza współrzędne środka x, y, długość i kąt nachylenia każdej wydzielonej mikroszczeliny. Następnie za pomocą arkusza kalkulacyjnego, oznaczono odległość każdej wydzielonej mikroszczeliny od makroskopowej powierzchni pęknięcia, stanowiącej początek profilu pomiarowego. Określono również kąt nachylenia dla każdej wydzielonej mikroszczeliny względem powierzchni pęknięcia makroskopowego. Na podstawie uzyskanych danych wykonano zbiorcze wykresy liczebności, długości i kierunków rozprzestrzenienia mikroszczelin w funkcji długości profilów pomiarowych.

W oparciu o analizę wyników badań stwierdzono co następuje:

1. Zwiększające się ciśnienie okólne $\sigma_3 = \sigma_2$ i odkształcenie podłużne próbki ε_1 powoduje wzrost liczby mikroszczelin.
2. W próbce nr 1 ($\sigma_3 = \sigma_2 = 200$ MPa i $\varepsilon_1 = 5\%$) zarejestrowana liczba mikroszczelin w początkowej części profilu pomiarowego (bezpośrednie sąsiedztwo powierzchni poślizgu) jest znacznie większa niż w dalszej jego części.
3. W próbce nr 2 i nr 3 ($\sigma_3 = \sigma_2 = 300$ MPa i $\varepsilon_1 = 10\%$ oraz $\sigma_3 = \sigma_2 = 300$ MPa i $\varepsilon_1 = 15\%$) mikropęknięcia i mikroszczeliny rozprzestrzeniają się i obejmują znaczną objętość próbki, toteż ich liczebność w funkcji długości profilu pomiarowego nie wykazuje większego zróżnicowania.
4. Zwiększenie ciśnienia okólnego i skrócenia osiowego próbek wpływa na wzrost sumarycznej długości pomierzonych mikroszczelin.
5. Kierunki rozprzestrzenienia mikroszczelin względem powierzchni poślizgu w trzech seriach pomiarowych są do siebie zbliżone.

Słowa kluczowe: ciśnienie okólne, górotwór, powierzchnia poślizgu, mikropęknięcia, naprężenie, odkształcenie

1. Introduction

Discontinuous deformation structures such as fractures and fissures, forming in rock medium ought to be examined both in microscopic scale (of the size of grains) as well as macroscopic one. In fact, it is in microscopic scale where the process of destructing structure of rock begins through initiation and propagation of microcracks, which further by combining with each other into systems or complexes of fractures lead to macroscopic destruction of rock structure. Microscopic observations of rocks examined in conditions of conventional triaxial compression (axial – symmetrical state of stress $\sigma_1 > \sigma_2 = \sigma_3$) in a wide range of confining pressures σ_3 (0÷400 MPa) allow to analyse versatility of the process of initiation and propagation of fractures which leads to destruction of rock structure depending on the state of stress.

In this article, a method for determination of microscopic structures of deformation is presented which has been developed in samples of sandstone from Tumlin during conducted tests of strength in triaxial state of stress. Adopted by the author, method of computer analysis of image allowed to carry out detailed examinations of the number, length and directions of propagation of microcracks against macroscopic surface (destruction) of slip in sandstone samples.

2. Influence of the value of confining pressure on the development of discontinuous deformations in the Tumlin Sandstone

For the research, sandstone was adopted which occurs in the northern part of the margin of Świętokrzyskie Mountains (the Holy Cross Mountains) and forming lithostratigraphic unit called strata from Tumlin – the Middle Buntsandstein (Senkowiczowa & Ślączka, 1962). Complex of laminated Tumlin sandstones reaches depth of about 200 m and is made of layers of sandstone of thickness from 2 to 3 m – of eolian origin, as deposits of dunes and interdune hollows.

Sandstone is characterized with variance of colour, from red-brownish to light brown, fine- and medium-grained as well as siliceous-ferruginous-clay binding agent of contact-porous and regenerative type. The main constituent of rock are well rounded, in part highly angular grains of quartz of diameter from 0.1 to 1.0 mm (on average 0.5 mm), coated with iron oxide-hydroxide. Subordinate group of minerals characterized with high level of roundness constitute grains tourmaline, apatite, amphibole, zircon, rutile and garnet. According to Pettijohn's petrographic classification the analysed rock is sublithic arenite (Pinińska, 1994).

In the complex of sandstone there are fractures and fissures of length from a few cm to a few meters, and their spread oscillates from a few to several dozen centimetres. According to Mencel's classification fractures and fissures form geometrical array of fractures Y, K type. However, linear, surface and spatial fracturing of sandstone massif amounts to: 4/m, 1.9 m/m^2 and 3.9 m^2/m^3 respectively (Pinińska, 1994).

Characteristic feature of sandstones is their very good divisibility, which enables extraction of sandstone plates of any thickness and large size. Owing to its favourable pysio-mechanical parameters, the Tumlin Sandstone is a valuable and searched for raw material on the market.

Testing of mechanical properties of the Tumlin Sandstone was performed in the Strata Mechanics Research Department of the Strata Mechanics Research Institute (Polish: Instytut Mechaniki Górotworu PAN) in Krakow. Strength testing of sandstone was conducted on apparatus GTA – 10 with confining pressure ranging from 0 to 400 MPa on cylindrical samples with diameter of 22.5 mm and twice as bigger height (slenderness ratio 2).

Samples of sandstone were initially subjected to omni-directional hydrostatic stress $\sigma_1 = \sigma_2 = \sigma_3$, which corresponded to the applied confining pressure, and then at constant value of this pressure, samples were lowered with axial force to the value of longitudinal strain applied beforehand. Testing was conducted in several cycles. One cycle included carrying out investigations for four samples of sandstone at constant confining pressure and applied in advance variable longitudinal strain different for each sample amounting to 5%, 10%, 15% and 20%. After the sample reached the required longitudinal strain, it was lightened to zero value of differential stress and then it was taken out from the pressure chamber of the apparatus and was thoroughly examined and photographed. As a result of an experiment curves of dependency between differential stress, longitudinal and transverse strain of the sample were received. Longitudinal strain was determined on the basis of the position of piston pressing the sample, while transverse strain was determined by means of measurement with inductive sensor, girding the sample half its height, according to the way described by Nowakowski and Nurkowski (1995).

In Figure no. 1, a characteristic abrupt increase of the value of differential stress $\sigma_1 - \sigma_3$ is visible for confining pressure σ_3 over 200 MPa, which corresponds to the pressure of transition from brittle fracture to ductile strains of the rock. The interval between these states and corre-

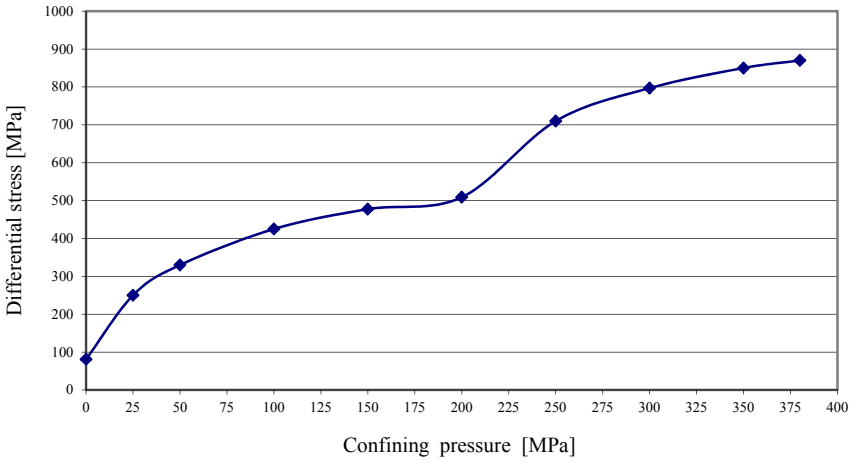

Fig. 1. Dependence between differential stress corresponding to ultimate strength of the sample and confining pressure (based on research by J. Guskiewicz); the Tumlin Sandstone

sponding to them pressures is relatively narrow and results from the fact that friction force on macroscopic surface of shearing becomes larger than ultimate strength on compression of the rock (Gustkiewicz, 1999).

Presented in Figure 2, maximum values of stress are ultimate strengths of rock at applied confining pressures, and deformations corresponding to them are deformations on ultimate strength. From the course of curves it arises that with increasing confining pressure increases strength of the sample and corresponding to it longitudinal strains and transverse strains. Curves marked with number 25, 50, 100, 150, 200 show rapid fall of strength, connected with brittle fracture of the rock. However, the course of curves described with numbers 250, 300, 350 and 400 after exceeding ultimate strength settled on a certain, for a given confining pressure, level and is connected with ductile strains of rock.

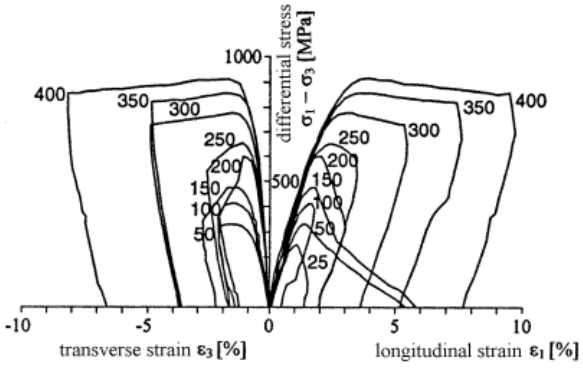

Fig. 2. Dependence between differential stress and longitudinal and transverse strains for confining pressure in (MPa) as a parameter (according to Gustkiewicz); "Tumlin" Sandstone

For confining pressures – below 200 MPa samples displayed brittle cracking, and fissure was preceded with elastic deformations and inconsiderable permanent deformations. This fissure was rapid was accompanied by acoustic effects (acoustic emission was not a subject of the research).

For confining pressures – above 200 MPa – samples were characterized with ductile character of destruction, but before they started to crack, reached considerable strain. With the developing longitudinal strain, occurred evenly distributed two systems of surface of shearing. These systems thickened with the increase of strain, and starting from its certain value, appeared two coupled shear surfaces running through the whole sample.

3. Study of development of microscopic structures of deformation in the Tumlin Sandstone depending on the value of confining pressure and longitudinal contraction of samples

In order to preserve deformations (fractures and fissures) formed in samples of sandstone during strength testing in triaxial state of stress, samples have been properly protected and bonded with epoxy resin. Epoxy resin of blue tint colour, migrating through the structure of rock samples filled in hollows – pores, fractures and fissures formed during triaxial testing. After bonding, sandstone samples were cut into fragments – slices (thickness of a few millimetres), in parallel to vertical axis of samples, then they were abraded to thickness of 35÷40 μm. After obtaining suitable thickness of slices, microscopic sections were prepared from them. In total 49 microscopic sections were made of samples of sandstone tested in diversified states of stress-strain. Microscopic testing of a wide range of sections was performed by the author with the use of optical microscope of "Olympus" company integrated with digital camera. For characteristic regions within microscopic sections a series of colour photographs in 25- and 100-tuple enlargement was taken.

Two types of failure of rock material were distinguished on the basis of the analysis of development of microscopic deformation structures in sandstone samples.

The first type of failure occurs in the sandstone samples examined in the following states of stress-strain: $\sigma_3 = 125$ MPa – $\varepsilon_1 = 20\%$ $\sigma_3 = 150$ MPa – $\varepsilon_1 = 2{,}5\%$ as well as $\sigma_3 = 200$ MPa – $\varepsilon_1 = 5\%$ and is characterized by visible single fissure (Pic. 1 and 2) running between upper and lower base of the sample inclined at angle of 30-35° against the direction of the main stress. This type of failure occurred as a result of shearing and displacement of rock material along the surface of fracture. About the existing strike-slip movement signify numerous comminuted (crushed) chippings of grains of quartz and binding agent lying within the surface of fracture (Pic. 2). Width of the surface of fracture is variable and ranges from 150 to 400 μm. Along the surface of fracture, on both of its sides, there is a zone with microcracks and microfissures. In this zone, structures of deformation demonstrate orientation close to vertical axis of the sample, but also form clusters characterized with changeable direction of deposition.

Above the value 200 MPa of confining pressure, changes the character of failure of sandstone samples. There occur single ($\sigma_3 = 300$ MPa – $\varepsilon_1 = 5\%$ and $\sigma_3 = 300$ MPa – $\varepsilon_1 = 10\%$) or double ($\sigma_3 = 250$ MPa – $\varepsilon_1 = 10\%$) intensively fractured zones in a form of strips (Pic. 3 and 4) running between lower and upper base of sandstone sample. The width of single intensively fractured

Pic. 1. Sample's cracking, microscopic section (σ_3 = 125 MPa; ε_1 = 20%)

Pic. 2. Sample's cracking (σ_3 = 125 MPa; ε_1 = 20%), enl. × 25

Pic. 3. Zone of destruction of the sample, microscopic section (σ_3 = 250 MPa; ε_1 = 10%)

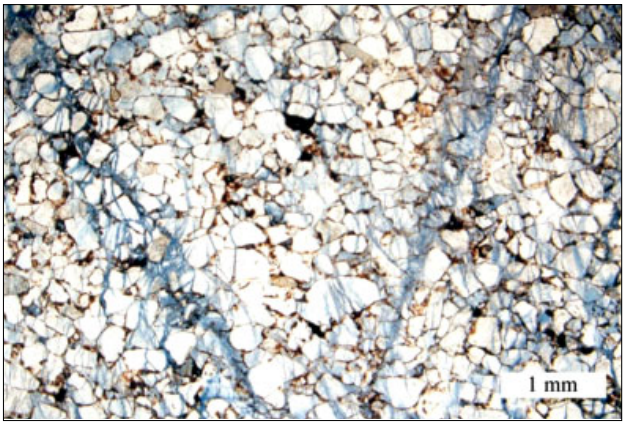

Pic. 4. Failure zones of sample (σ_3 = 250 MPa; ε_1 = 10%), enl. × 25

zones amounts to 160 μm (σ_3 = 300 MPa – ε_1 = 5%) and 200 μm (σ_3 = 300 MPa – ε_1 = 10%) and their inclination angle against vertical axis of sample amounts to 20° and 35° respectively. Whereas, the width of the two coupled intensively fractured zones (strips) takes the value of about 400 μm and their inclination against vertical axis of the sample is 20° and 30°.

The difference between the two types of destruction became visible also in abundance and the range of microcracks and microfissures occurring in the vicinity of the surface of fractures and intensively fractures zones (strips).

In the first type of failure, parts of material not covered in fissure are free from failure, only in immediate vicinity of the surface of shearing occur microcracks and microfissures.

In the second type of failure, formed intensively fractured zones, can hold the opposite sides of the material in cohesion. Clusters of microcracks and microfissures visibly propagate in substantial volume of the sample.

On the basis of research it has been found that the angle of inclination of the surface of fractures against the base of sample decreases with the increase of confining pressure. This peculiarity has been described by Gustkiewicz (1999) investigating sandstones from the Vosges.

For testing of microscopic structures of deformation with a method of computer analysis of image, three samples of the Tumlin Sandstone were selected (three microscopic sections), representing the following stress-strain states:

sample no. 1 (σ_3 = 200 MPa confining pressure and ε_1 = 5% longitudinal strain),
sample no. 2 (σ_3 = 300 MPa confining pressure and ε_1 = 10% longitudinal strain),
sample no. 3 (σ_3 = 300 MPa confining pressure and ε_1 = 15% longitudinal strain).

On the basis of carried out microscopic observations, areas with characteristic zones of fracture formation were marked off for the above mentioned sections and a series of colour images forming measurement cross section was taken of them. In measurement cross sections registered microfissures occurring both inside and outside grains of quartz and within the binding agent. Picture was taken in 100-tuple enlargement perpendicular to vertical axis of sample, so that their coming into contact with each other included constant transition from areas free from fractures or areas slightly damaged into zones with fractures covering slip surface. Measurement cross sections included in their scope fragment of the surface of microscopic section with length of about 11 mm and height of 1.0 mm.

In the image, the following structures of deformation have been distinguished (Pic. 5).

Preparation of input data for computer analysis was carried out in two stages. In the first stage, the picture from measurement cross sections was scanned and then by means of Photo Shop programme structures of discontinuous deformations were marked off. Below (Pic. 6a) there is

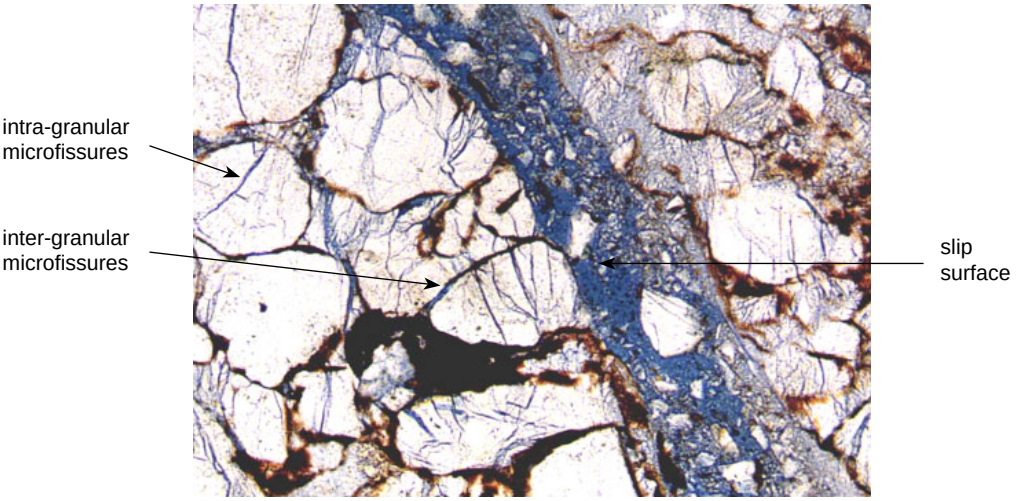

Pic. 5. Components of image

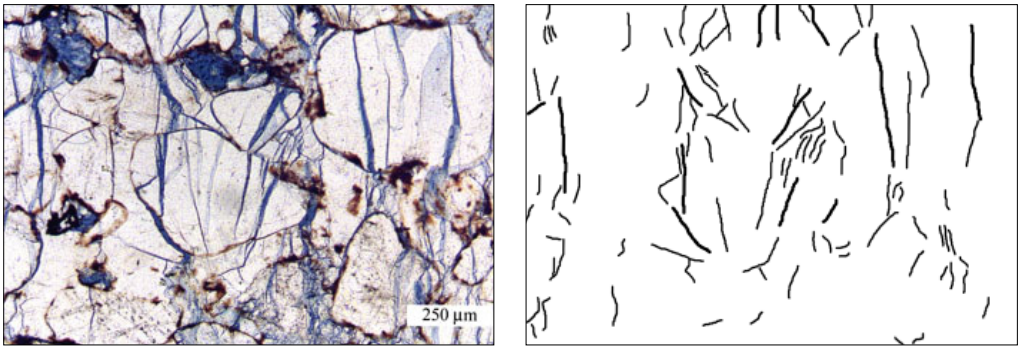

a) b)

Pic. 6. a – photograph of microfissures, b – marked off microfissures

a picture taken in 100-tuple enlargement with visibly marked microfissures (in blue). Another picture (Pic. 6b) illustrates separated microfissures.

At the second stage with the use of the programme Scion Image for the total of separated microfissures the following parameters were determined (Fig. 3 and 4).

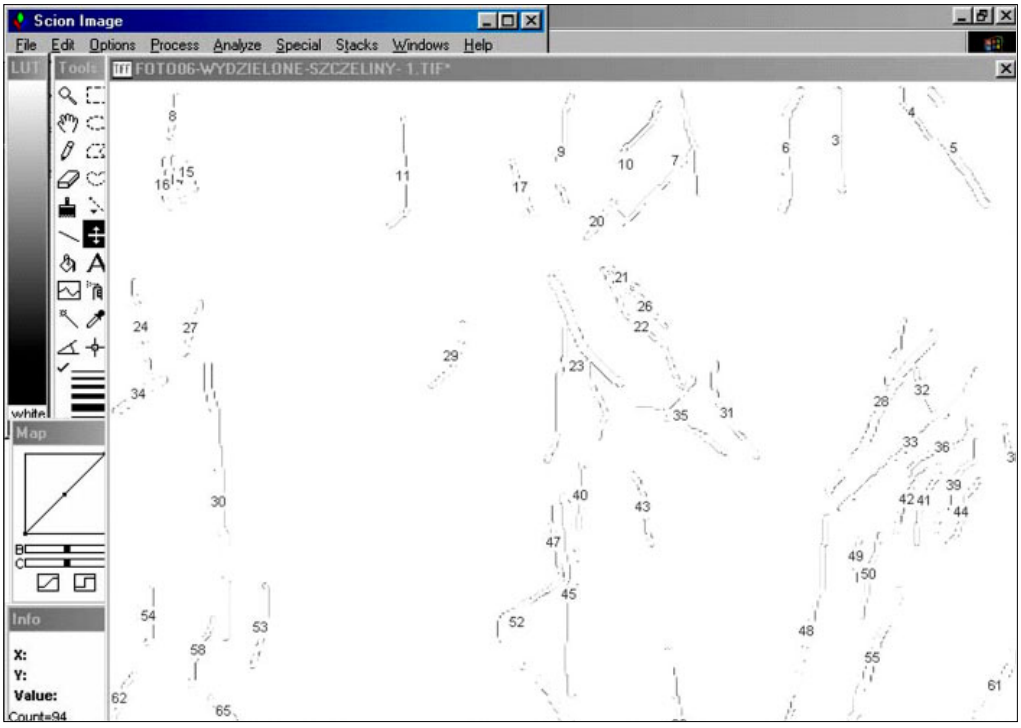

Fig. 3. Fragment of processed picture showing numeration of fissures

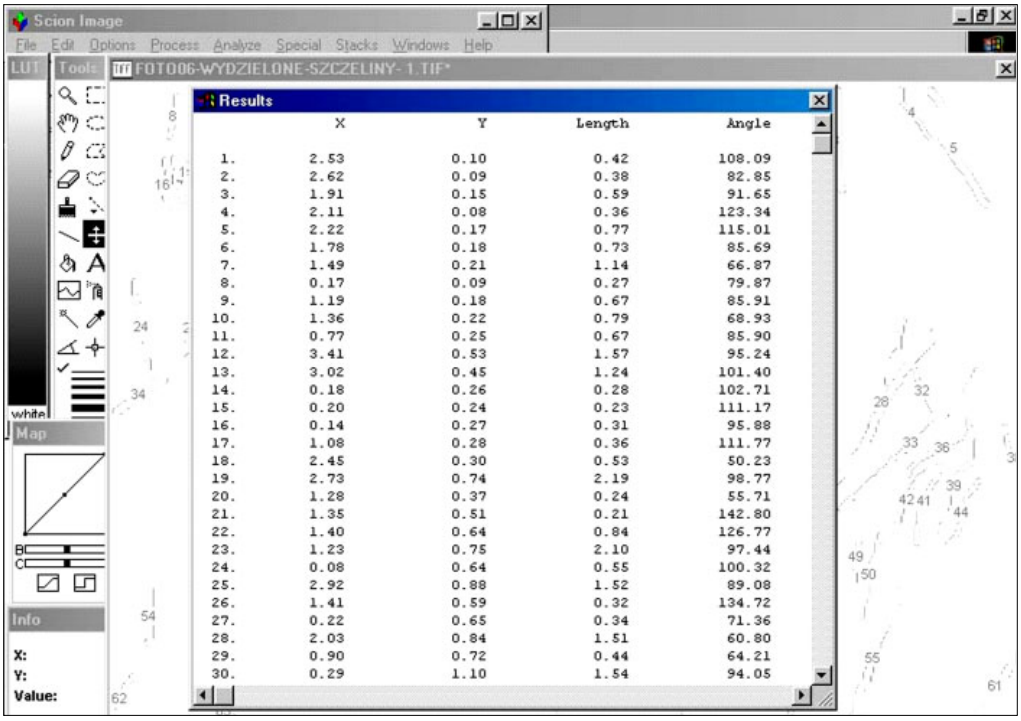

Fig. 4. Results of calculations: numeration, coordinates X, Y, lengths and angles of microfissures inclination

- reference number of microfissure,
- coordinates x, y of microfissure's middle,
- length of microfissure,
- value of angle included between directions of microfissures deposition and slip surface

Afterwards, with the use of spreadsheet, distance of separated microfissures from macroscopic surfaces of fracture was calculated (beginning of measurement cross section) as well as angles of inclination of microfissures against the surface of macroscopic fracture were determined. Subsequently, cumulative graphs were produced sowing number, length and directions of propagation of microfissures in a function of length of measurement cross sections.

4. Results of investigation of microscopic structures of discontinuous deformations

The presented examination results of microscopic structures of deformation have been determined for three samples of sandstone (three microscopic sections) representing the following stress-strain states:

sample no. 1 (σ_3 = 200 MPa confining pressure and ε_1 = 5% longitudinal strain),
sample no. 2 (σ_3 = 300 MPa confining pressure and ε_1 =10% longitudinal strain),
sample no. 3 (σ_3 = 300 MPa confining pressure and ε_1 = 15% longitudinal strain).

An analysis was made on the basis of variability of directions of propagation, abundance and length of microfissures in a function of the length of measurement cross section (Wadas, 2004). Test results have been presented graphically in a form of cumulative graphs (Fig. 5, 6 and 7).

Number of microfissures increases with the increase of confining pressure and axial deformation of samples and reaches from 508 in sample no. 1 (σ_3 = 200 MPa and ε_1 = 5%) to 1112 in sample no. 3 (σ_3 = 300 MPa and ε_1 = 15%). In the distance to about 2 mm (sample no. 1 and 2) and 3 mm in sample no. 2 (σ_3 = 300 MPa and ε_1 = 10%) from the slip surface registered the increase of number of microfissures (Fig. 5). Moreover, distribution of number of microfissures in particular samples shows considerable diversification. In the first sample, in the distance within 2 to 6 mm from the surface of slip, number of microfissures does not display greater diversity; however, in the further part of measurement cross section their number generally falls. In the second sample, in the distance from 3 to 8 mm from the slip surface registered a fall, and in the further part of the section – increase of number of microfissures. In the third sample, at the whole length of section registered high level of abundance of microfissures with local drops in their amount.

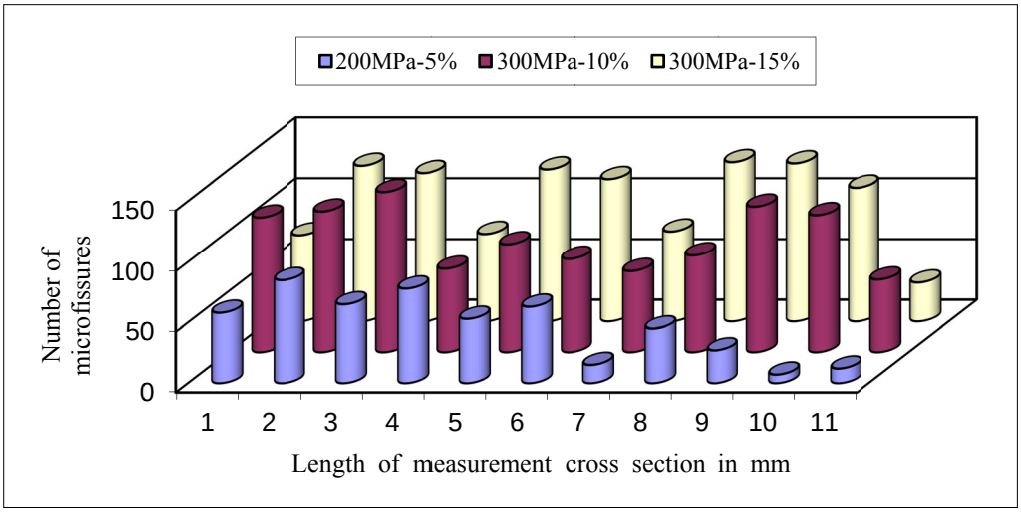

Fig. 5. Number of microfissures in sample no. 1, 2 and 3

On the basis of classification of microfissures lengths (Fig. 6) it can be stated that, their predominant number falls within the following length ranges: 20-110 µm (sample no. 1), 20-120 µm in (sample no. 2) as well as 20-90 µm (sample no. 3). Maximum number of microfissures registered in unitary length ranges 40-50 µm (sample 1, 2 and 3).

Directions of microfissures propagation microfissures against slip surface were included mainly in angle range from –10° to 80° (sample no. 1 and 2) as well as from –10° to 90° (sample no. 3). The maximum number of microfissures was registered in unitary angle range of 30°-40° (sample no. 1 and 3) as well as 20°-30° (sample no. 2) Fig. 7.

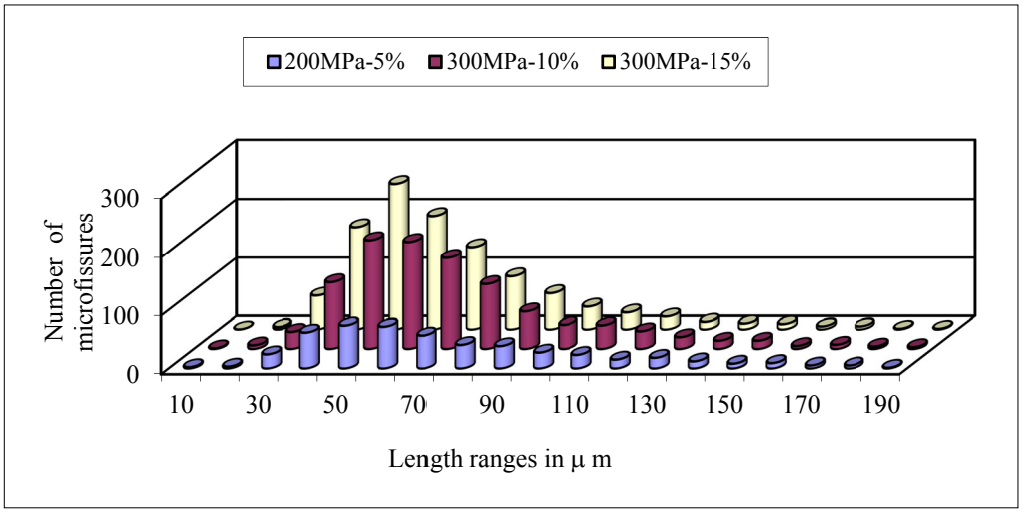

Fig. 6. Classification of microfissures lengths

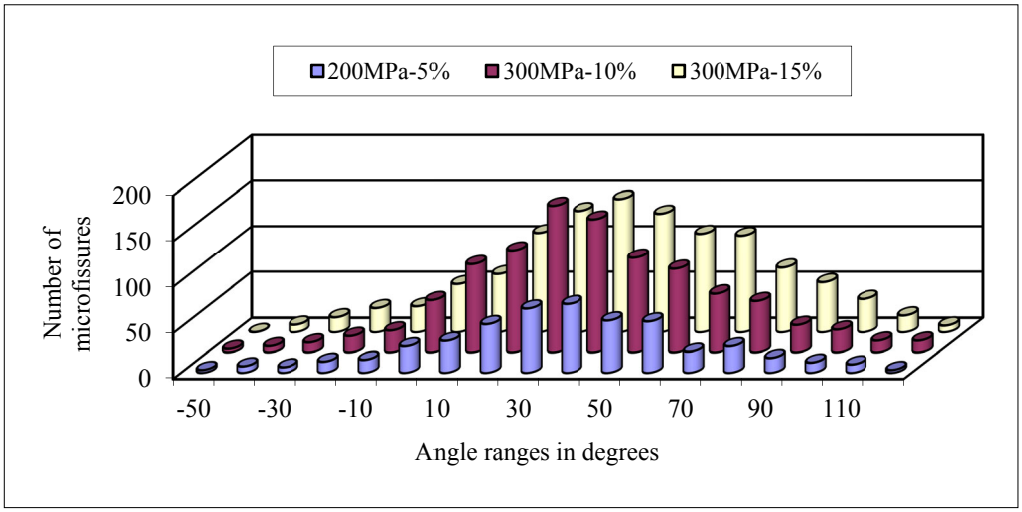

Fig. 7. Directions of microfissures propagation microfissures in sample no. 1,2 and 3 against slip surface

5. Summary

In the article a method of analysing discontinuous structures (fractures and fissures) occurring in rock samples during strength tests (triaxial) and determining zones of their range is discussed. The method of microscopic examination, worked out by the author, is based on application of computer analysis of image and allows to determine coordinates, length and angles of micro-

cracks and microfissures inclination in selected fragment of microscopic section. Working out the method enabled to investigate development of deformation structures (microfractures and microfissures) and range of their occurrence versus macroscopic surfaces of fractures. Testing was performed on selected three microscopic sections prepared from three samples of the Tumlin Sandstone, including the following stress-strain states:

sample no. 1 (σ_3 = 200 MPa confining pressure and ε_1 = 5% longitudinal strain),
sample no. 2 (σ_3 = 300 MPa confining pressure and ε_1 = 10% longitudinal strain),
sample no. 3 (σ_3 = 300 MPa confining pressure and ε_1 = 15% longitudinal strain).

On the basis of the obtained results of testing the following can be stated:

1. Increasing confining pressure $\sigma_3 = \sigma_2$ and longitudinal strain of sample ε_1 causes increase of the number of microfissures (Fig. 5) from 508 in sample no. 1 (σ_3 = 200 MPa and ε_1 = 5%) through 1034 in sample no. 2 (σ_3 = 300 MPa and ε_1 = 10%) to 1112 in sample no. 3 (σ_3 = 300 MPa and ε_1 = 15%).
2. In sample no. 1 ($\sigma_3 = \sigma_2$ = 200 MPa and ε_1 = 5%) registered number of microfissures in initial part of measurement cross section (close vicinity of slip surface) is considerably bigger than in its further part (Fig. 5).
3. In sample no. 2 and 3 ($\sigma_3 = \sigma_2$ = 300 MPa and ε_1 = 10% as well as $\sigma_3 = \sigma_2$ = 300 MPa and ε_1 = 5%) microcracks and microfissures propagate and encompass considerable volume of the sample, that is why their number in the function of length of measurement cross section does not display greater diversification (Fig. 5).
4. Increase of confining pressure and axial contraction of samples has influence on the increase of total length of measured microfissures (Fig. 6).
5. Directions of propagation of microfissures versus slip surface in three samples are similar to each other (Fig. 7).
6. Angle of inclination of slip surface against vertical axis of samples increases with the increase of confining pressure and amounts from 30° in sample no. 1 (σ_3 = 200 MPa and ε_1 = 5%) to 35° in sample no. 2 (σ_3 = 300 MPa and ε_1 = 10%) and no. 3 (σ_3 = 300 MPa and ε_1 = 15%).

Extension of study over the mechanism of forming fractures can provide an opportunity not only cognitive, but for practical utilization of research results in the scope of forecasting and explaining initiation processes of the state of rockburst hazard, in particular in regions of tectonic disturbance – faults, but also determination of influence of fractures on strength parameters of rocks, which is significant for selecting supports. Further research over development of discontinuous deformation structures as well as over the mechanism of their occurrence may also find application in works connected with designing and constructing of geotechnical structures (road, tunnel construction purposes) and hydro-geological (building dams).

References

Gustkiewicz J. i in., 1999. *Własności fizyczne wybranych skał karbońskich Górnośląskiego Zagłębia Węglowego*. Wyd. IGSMiE PAN, Kraków.

Nowakowski A., Nurkowski J., 1995. *A new method of measuring circumferent ial displacement in a triaxial cell*. Int. J. Rock Mech. Min. Sci. Geomech. Abstr., vol. 32, No 1, p. 65-70.

Pinińska J. i in., 1994. *Właściwości wytrzymałościowe i odkształceniowe skał. Część I. Skały osadowe regionu świętokrzyskiego – Informatyczne karty dokumentacyjne odsłonięć*. Wyd. Zakład Geomechaniki UW, Warszawa

Senkowiczowa H., Ślączka A., 1962. *Pstry piaskowiec na północnym obrzeżeniu Gór Świętokrzyskich*. Rocznik Pol. Tow. Geol., T. 32, nr 3. Warszawa.

Wadas M., 2004. *Zastosowanie komputerowej analizy obrazu fotograficznego w badaniach rozwoju mikroskopowych struktur deformacyjnych*. XXVII ZSMG. Geotechnika i budownictwo specjalne 2004. T. I. Wyd. KGBiG, AGH, Kraków.

Received: 11 January 2012